The Journal of Experimental Biology 204, 2431–2438 (2001)
Printed in Great Britain © The Company of Biologists Limited 2001
JEB3302

MICROSPECTROPHOTOMETRIC MEASUREMENTS OF VERTEBRATE PHOTORECEPTORS USING CCD-BASED DETECTION TECHNOLOGY

CRAIG W. HAWRYSHYN*, THEODORE J. HAIMBERGER AND MARK E. DEUTSCHLANDER‡
Department of Biology, University of Victoria, PO Box 3020 STN CSC, Victoria, British Columbia, Canada V8W 3N5
*Author for correspondence (e-mail: chawrysh@uvic.ca)
‡Present address: Rochester Institute of Technology, Rochester, NY 14623-5603, USA

Accepted 19 April 2001

Summary

We have developed a charge-coupled-device (CCD)-based microspectrophotometer (MSP) system and provide the first report on the successful employment of this technology to measure the spectral absorbance properties of vertebrate photoreceptors. The principal difference between the CCD-based MSP system and wavelength-scanning MSP systems, commonly used in vision biology, is that a short duration (800–1200 ms), broad-spectrum flash is employed rather than ascending and descending wavelength scanning. Data acquisition is thus significantly faster, with the added possible advantages of less variance due to movement of target photoreceptors during measurement, reduced spectral distortion due to photoproduct interference and an ability to measure fast, transient changes in absorbance as bleaching proceeds. Rainbow trout photoreceptors, previously measured with a wavelength-scanning MSP system, were again measured using the CCD-based MSP system. Our analysis of optical recordings from 102 photoreceptors corroborated data obtained previously with rainbow trout photoreceptors on λ_{max} (wavelength of maximum absorbance), A_{max} (maximum absorbance) and half maximum bandwidth (HBW) of ultraviolet-, blue-, green- and red-sensitive cones and rods. There were slight differences in λ_{max} and half-maximum bandwidth of the ultraviolet-, blue- and green-sensitive cone classes, but this was most probably due to variation in the A_1:A_2 visual pigment ratio of the trout used in the two different studies. However, we were capable of resolving the A_1 and A_2 visual pigment spectra in the red-sensitive cones and the rods.

Key words: CCD-based microspectrophotometer, photoreceptor, spectral absorption, rainbow trout, *Oncorhynchus mykiss*.

Introduction

Microspectrophotometry (MSP) is a well-established and effective method for studying the spectral absorption properties of photoreceptors. Two groups led by Edward F. MacNichol Jr. and Paul Liebman led the development of this technique in the early 1960s, making some of the first optical recordings from vertebrate cone photoreceptors (Liebman and Entine, 1968; Marks and MacNichol, 1962; Marks, 1965). Since this pioneering effort, MacNichol and other prominent research groups (e.g. Bowmaker, 1984; Bowmaker, 1990; Bowmaker, 1995; Loew, 1995; Loew and Dartnall, 1976; Liebman, 1972; Partridge, 1989; Sillman et al., 1997) have been successful in utilizing MSP to characterize the spectral absorption properties of photoreceptors over a broad range of fauna. MSP has played an important role in the discovery and subsequent taxonomic survey of ultraviolet-sensitive photoreceptors in vertebrates (Avery et al., 1983; Bowmaker and Kunz, 1987; Hárosi and Hashimoto, 1983; Hart et al., 1998; Hawryshyn and Hárosi, 1991; Hawryshyn and Hárosi, 1994; McFarland and Loew, 1994; Maier and Bowmaker, 1993). This technique continues to be one of the most important tools in the examination of ultraviolet photoreception, so it is with this utility in mind that we introduce CCD-based MSP as a new and potentially significant development.

To date, most, if not all, MSP systems used in examining vertebrate photoreceptors are designed to measure the transmitted light flux through photoreceptor outer segment (sample spectrum) and a clear area of the field (reference spectrum), as the spectrum is scanned (at 300–800 nm wavelength). Absorbance values ($\log T^{-1}$) (T, transmittance) are calculated as a function of wavelength in regular wavelength increments (e.g. 5 nm; Harosi, 1987). The measurement time required to traverse the spectrum, usually in both an ascending and a descending series, varies from one apparatus to another. Linear diode arrays have been used to measure the spectral absorbance of photoreceptors with some degree of success (Widder et al., 1987; Hiller-Adams et al., 1988), but spectral absorbance curves presented in these papers consistently show a discordance with Dartnall nomogram templates. With the rapid development of electro-optical technology, CCD (charge-coupled device) chip technology has been used recently with success in a wide variety of

spectroscopic applications (Maseide and Rofstad, 1997; Schweitzer et al., 1996; Tang et al., 1994; Tsujita et al., 1997). One of the important features of CCD chip technology is that it is comparatively fast (800 ms per scan and only one scan required) relative to wavelength-scanning MSP systems (up to 10 s per scan with multiple scans but there are appreciable differences between each MSP apparatus). This is possible because our CCD-MSP system uses one flash of full-spectrum light (300–800 nm) with a short-duration (800 ms). The transmitted flux is measured by a CCD detector used in tandem with a high-resolution (0.4 nm) spectrograph, providing the same information as a MSP system in a much shorter period of time. The rapid measurement time may have important implications when measuring fragile retinal tissue. For instance, excised salmonid retina is only viable for approximately 1 h. With a shorter measurement time, more cells can be measured at the peak quality of the tissue. Furthermore, photoreceptor movement in retinal preparations, even for the most stable preparations, can account for considerable signal variance, and rapid signal acquisition therefore should help to minimize signal variance.

In this paper, we describe the design of the CCD-based MSP instrument and offer some thoughts on overcoming problems inherent to the technology. We also evaluate the performance of the instrument using rainbow trout (*Oncorhynchus mykiss*) retinas, previously measured (Hawryshyn and Hárosi, 1994) using the wavelength-scanning MSP system.

Materials and methods

Animals and care

Wild stock rainbow trout *Oncorhynchus mykiss* (Walbaum) parr (5–30 g body mass) were obtained from Fraser Valley Hatchery, Abbottsford, British Columbia, Canada. They were held at a mean water temperature of 15±1 °C and a photoperiod of 12 h:12 h L:D (standard fluorescent light) in the Aquatic Facility of the University of Victoria. Fish were fed trout pellets on a daily basis, *ad libitum.* All procedures and care were in accordance with the University of Victoria Animal Care Committee, under the auspices of the Canadian Council for Animal Care.

Tissue preparation

After overnight (or at least 2 h) dark adaptation, fish were anaesthetized by immersion in Tricaine methanosulphonate (MS-222, Cresent Chemicals) (300 mg l^{-1}) for approximately 10 min and then killed by cervical transection. The eyes were removed and hemisected under near infrared illumination provided by light-emitting diodes (LEDS) with a peak output at 660 nm. The retinae were removed using forceps and placed in a cell culture dish containing freshly prepared, ice-chilled Minimum Essential Medium (MEM; Sigma). 292 mg l^{-1} L-glutamine and 350 mg l^{-1} $NaHCO_3$ were added, the pH adjusted to 7.3 using 1 mol l^{-1} NaOH, and the solution filtered through a 0.22 µm filter. The dish was kept in a light-tight container placed on ice. Illumination was provided by infrared LEDs (primary wavelength of emission 880 nm). A piece of retina was sectioned using a razor blade segment under infrared LEDs and placed on a coverslip. A razor blade was used to cut the retina section into many small pieces. This provided better preparations than could be attained by teasing the tissue with forceps. MSP recordings were collected at a constant temperature of 15 °C.

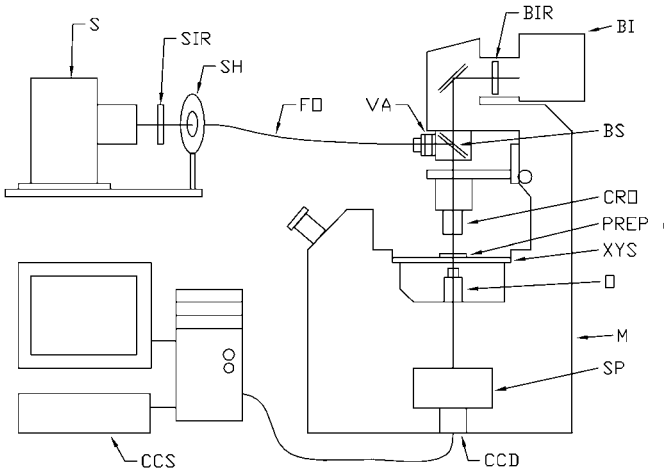

Fig. 1. Schematic diagram of the CCD microspectrophotometer. BI, back illumination; BIR, infrared filter; BS, beam splitter; CCD, charge-coupled device camera; CCS, custom computer software; CRO, reflective objective as condenser; FO, fibre optic cable; M, microscope; O, objective lens; PREP, preparation; S, xenon lamp (light source); SH, shutter; SIR, infrared filter mounted on a swing arm; SP, spectrograph; VA, *X–Y* variable aperture; XYS, *X–Y* stage.

Microspectrophotometer design

Fig. 1 shows a schematic layout of the experimental apparatus. The measurement beam light source was provided by a 150 W xenon arc lamp (Oriel) equipped with a condenser lens system that was adjusted to focus on the plane of the shutter. A light intensity controller (Oriel) is currently being added because of small transient fluctuations in intensity, which can lead to spurious noise in the signal. To enable the measurement beam to be positioned without undue bleaching of the preparation, an infrared filter (Ealing Far Red, Schott RG850 or RG1000), attached to a swing arm, was moved in and out of the path of the light beam situated in front of the shutter position. A quartz disc diffuser was mounted at the shutter (Uniblitz) plane to blur the arc image. A quartz fibre-optic cable (Voltrex) fed light from the shutter onto an *X–Y* variable slit aperture (Leitz), then to a beam-splitter mounted in a cube on the Zeiss Axiovert TV100 inverted microscope above the condenser lens [Ealing 52×, 0.65 numerical aperture (NA) mirror objective]. The condenser lens system formed an image of a variable slit aperture (Leitz). The measurement beam used in the recordings presented in this paper was unpolarised. The background illumination was provided by a 12 V, 100 W halogen lamp on the Axiovert microscope. An Ealing Far Red, Schott RG850 or RG1000 filter was placed in the background channel to prevent bleaching of photoreceptors. A second CCD camera (Canadian Photonics Laboratory), mounted on the trinocular (not shown in Fig. 1), was used for

viewing the microscope field and was displayed on the computer monitor. This camera was used to capture infrared images of the preparation.

The original Zeiss condenser lens holder tended to show drift. It is now being replaced by a *X–Y–Z* stage with micrometer screws. The condenser lens was an Ealing reflecting objective (52×, 0.65 NA). While chromatic aberration is not a problem with reflecting objectives, alignment of the reflecting surfaces is critical. Two adjustment screws allowed for centering of the primary and secondary mirrors using a silver point slide provided by Ealing. An outer ring set the coverslip thickness and the distance from the objective to the entrance aperture of the spectrograph (set at infinity). An *X–Y* stage (Zeiss) with micrometer screws allowed positioning of the specimen relative to the measurement beam. The objective lens was a Zeiss Ultrafluor (100×, 1.20 NA, glycerine immersion objective lens). The optical path of the microscope was centered once per week using an alignment objective and eyepiece (Zeiss). A Spectra-Pro 300i (Acton Research Corporation), 300 mm focal length spectrograph, was used. It has a three-position turret with 150 g mm^{-1}, 300 g mm^{-1} (300 nm blazed) gratings and a mounted mirror. For maximum light intensity, the 150 g mm^{-1} grating was usually used. The CCD detector was a PI 1340, 400 pixel, CCD array with four-stage Peltier cooler (Princeton Instruments, Roper Scientific) operating at −50 °C.

CCD detector

After light has passed through the specimen, it enters the spectrograph. There, it is diffracted by an ultraviolet blazed grating, which acts to spread the light beam spectrally across the *X*-axis (columns) of the CCD chip. The CCD array used a chip with a pixel array of 1340 columns and 400 rows. Each pixel can be considered as a well in which charges accumulate when photons are absorbed. The voltage potential of each pixel rises as the number of charges increases. When the CCD is read, the charges are moved towards one side of the chip (electronically). It is possible to fetch each (of 400) rows of pixels individually or to let the charges accumulate in the exit row. The number of rows summed in the exit row (before it is dumped) can be set. This procedure is called vertical binning. Its usefulness is limited by the 16-bit (65536 level) resolution of the A/D converter, which allows a maximum value of 65535. The A/D converter converts the analog potential at the CCD exit row to a digital number.

A second characteristic of CCD chips is called the region of interest (ROI). The measurement beam is approximately 1 μm × 2 μm in size (adjusted by an *X-Y* variable slit system, Leitz) when it traverses the photoreceptor. The grating in the spectrograph spreads this rectangle across the CCD according to wavelength. This image does not cover the whole height of the CCD array. To eliminate noise originating from less well illuminated pixels of a column it is possible to restrict the dump from the CCD to specified rows or strips of rows. The rows selected belong to the ROI (region of interest). It is also possible, at a loss of wavelength resolution, to average columns. The ROI is specified by the range of rows to be dumped and by the number of columns to average.

Parameters of measurement

To measure the spectral absorbance of a photoreceptor two spectra were compared: a reference measurement was performed by placing the measurement beam in a clear tissue-free area and a photoreceptor measurement was performed by placing the measurement beam within the photoreceptor outer segment (background level was subtracted from all spectra collected). Absorbance was calculated as $\log_{10}$ of the ratio of the intensity of the reference spectrum over the intensity of the sample measurement spectrum.

To achieve the best signal-to-noise ratio (S/N), the exposure time is adjusted to provide pixel counts in the ultraviolet region of the spectrum that are well above background noise. For instance, with the use of vertical binning we have determined that a 0.8 s exposure time produces about 6000 counts at 340 nm and 400 000 counts at 700 nm. This exposure time is set to minimize photoreceptor bleaching. For the experiments described here, exposure times from 0.8 to 1.2 s in one flash proved optimal.

In the wavelength range below 350 nm, low source output was the main source of signal noise. We have added a light intensity controller (Oriel) to reduce the variability of the signal amplitude across the spectrum.

Calibration

Wavelength calibration of the CCD-MSP system was performed using spectral lines generated from both a xenon light source (Oriel) and a fluorescent lamp (RadioShack). This wavelength calibration is performed every 2 weeks. Optical density calibration was performed by comparing neutral density filters of known density with density measurements determined by the CCD-MSP system.

Software

The drivers for the CCD camera were provided by Roper Scientific as a dynamic link library (DLL). The graphical user interface (GUI) was written in Visual Basic (Microsoft). For plotting and mathematical analyses, a run time version of IDL (Research Systems, Inc) as an Active X control (software library/toolbox accessible from multiple software applications) was used.

Photoreceptors are refractive and thus, any displacement of the image of the measurement beam on the CCD detector can lead to a shift either along the wavelength axis or within the region of interest (leading to a shift in amplitude), or both. A shift along the wavelength axis between the reference and the measurement spectra introduces distortion into the absorbance spectrum. Because all recorded spectra exhibit spectral spikes or lines, the measurement spectrum can be shifted to coincide with the reference spectrum. This procedure of correcting for spectral pixel-shifting is required for approximately 30 % of the measurements performed.

Table 1. *Spectral data for rainbow trout photoreceptors examined in this study*

Photoreceptor type	Number of cells	Mean λ_{max} (nm)		Mean half-maximum bandwidth (cm^{-1})		Mean A_{max}		Mean outer segment diameter (μm)[6]		Specific absorbance (μm^{-1})[5]	
		Present[1]	Previous[2]	Present	Previous	Present	Previous	Present	Previous	Present	Previous
Ultraviolet-sensitive cones	11	371±9.2[3]	365±5[3]	5051±130[3]	4700±1200[3]	0.014±0.008[3]	0.015±0.006[3]	2.24±0.35[3] (7)	2.7±0.3[3]	0.00625	0.0086
Blue-sensitive cones	29	432±10.4	434±5	4329±112	6600±1500	0.01±0.005	0.019±0.005	2.75±0.66 (11)		0.00364	0.0102
Green-sensitive cones	25	519±8.5	531±6	3604±61.6	4400±500	0.013±0.005	0.023±0.005	3.26±0.48 (9)	3.9	0.00399	0.0079
Red-sensitive cones (A_1 based)	6	574±13.9	576±3	3256±79.4	3700±200	0.012±0.009	0.022±0.005	3.26±0.48 (9)	3.9	0.00368	0.0068
Red-sensitive cones (A_2 based)	8	623±17.8		3709±89[4]		0.022±0.012		3.26±0.48 (9)		0.00675	
Rods (A_1 based)	10	504±2.1		3661±46		0.017±0.009		1.94±0.62 (5)		0.00876	
Rods (A_2 based)	5	522±8.2	521±4	3762±551[4]	4400±300	0.014±0.003	0.037±0.017	1.94±0.62 (5)		0.00722	
Rods (A1-A2 mixed)	8	510±2.1		3881±380[4]		0.017±0.006		1.94±0.62 (5)		0.00876	

λ_{max}, wavelength of maximum absorbance; A_{max}, maximum absorbance.
All values are means ± 1 S.D.
[1]Values obtained from present study.
[2]Values are taken from Hawryshyn and Hárosi, 1994.
[3]All values are ±1 S.D.
[4]Estimates were derived from the Fourier transform fit.
[5]Specific absorbance is calculated by taking the ratio of mean A_{max} over mean outer segment diameter.
[6]Numbers of cells averaged are given in parentheses.

Acceptance criteria for spectra

The long-wavelength limb baseline was used as the first criterion. Since the photoreceptors are small and the absorbance weak, MSP data are inherently noisy, and strategies of analysis have been developed. For this publication, criteria of acceptance and methods of analyses were guided by Hárosi (Hárosi, 1987), MacNichol (MacNichol, 1986) and Levine and MacNichol (Levine and MacNichol, 1985).

If it was well defined, the spectrum was given further consideration. If it showed a clear linear trend (tilt) it was linearly detrended (Hárosi, 1987) and a template was then fitted to the data. For A_1-based visual pigment cones (vitamin A_1-based visual pigments are also called rhodopsin visual pigments; vitamin A_2-based visual pigments are also called porphyropsin visual pigments), an eighth-order polynomial (Bernard, 1987) was fitted to the absorbance spectrum and for the rods a long-wavelength limb chart (Munz and Beatty, 1965), characterized by λ_{max} and half-maximum bandwidth (HBW), was fitted to the long-wavelength limb of the absorbance spectrum. If the short- or long-wavelength limb of the spectrum was narrower or wider than the template, the spectrum was rejected. Lastly, for most photoreceptors it was also possible to acquire a bleached spectrum by exposing photoreceptors to the measurement beam for 120 s. This was used as an additional criterion for acceptance.

Cones

The fit of the eighth-order polynomial template provided λ_{max} and HBW for each spectrum. The spread in λ_{max} of the ultraviolet-, blue- and green-sensitive cones and their number of measurements were not large enough to try to group them according to porphyropsin content. This does lead to a less precise estimation of the HBW for these cones. The red-sensitive cones could be separated on the basis of visual pigment composition (i.e. those clustered around 570 nm for the A_1-based visual pigment and those clustered around 620 nm for the A_2-based visual pigment). Each group was normalized and averaged.

Rods

λ_{max} and HBW for rods containing rhodopsin, porphyropsin and mixtures of both, were known (Munz and Beatty, 1965). For each rod spectrum these two values were fitted. After normalizing, the rod data were divided according to porphyropsin content relative to rhodopsin concentration: less than 10 %, more than 80 % and approximately equal concentrations (40–60 %). Fish that contained a predominance of porphyropsin had a lower body mass in the size range used. The averages for each group were calculated and compared with published values (Munz and Beatty, 1965).

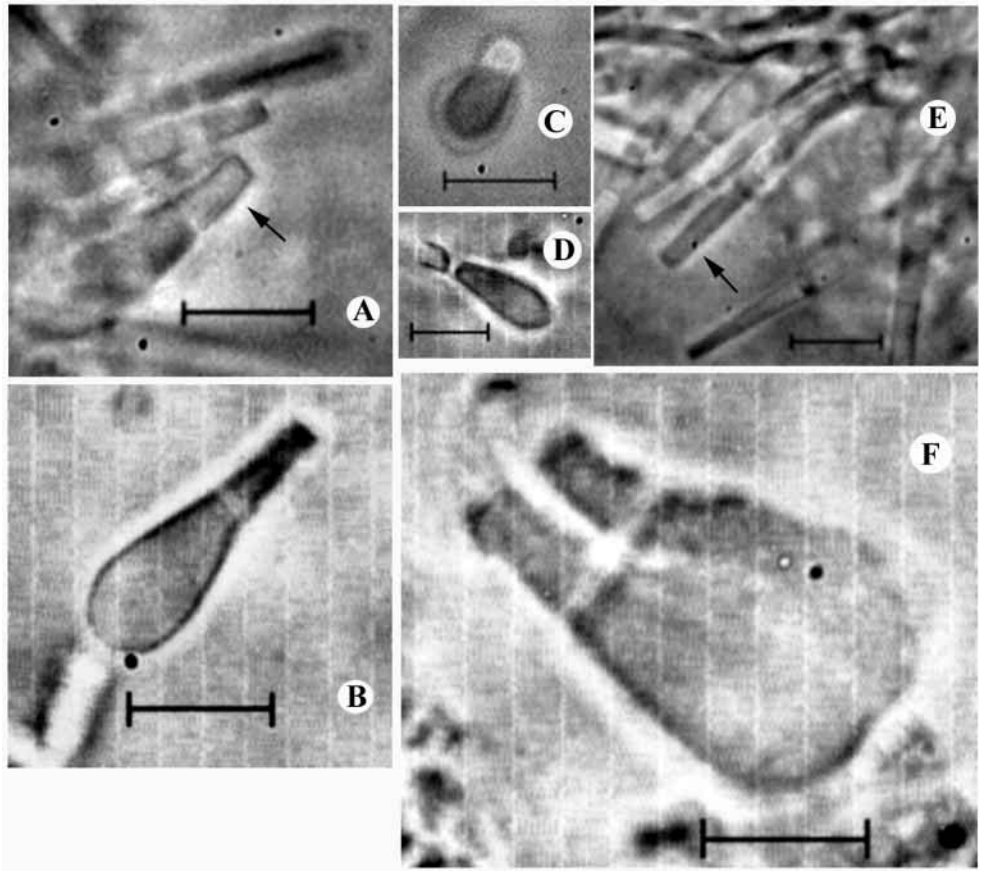

Fig. 2. Representative images of rainbow trout photoreceptors taken under infrared illumination. (A) The arrow points to a blue-sensitive cone (also shown in B and C). (D) Ultraviolet-sensitive cone. (E) Rod photoreceptors. (F) Double cone. Additional images were used in the calculation of mean outer segment diameter, which was used to determine specific absorbance (see Table 1). Scale bars, 10 μm.

Results

We recorded a total of 300 rainbow trout photoreceptors, of which 102 sets of spectral data were used in the final analysis with a distribution as follows: 40 single cones, 39 double cones and 23 rods. The data are summarized in Table 1 and data for comparison are provided, derived from measurements utilizing a wavelength-scanning MSP system (Hawryshyn and Hárosi, 1994). A collage of representative photoreceptor images is presented in Fig. 2. Infrared images were collected when possible and were used to provide dimensional information used in calculating specific absorbance (μm^{-1}) of the different spectral classes of photoreceptor (Table 1).

Single cones

Single cones measured in this study were either ultraviolet- or blue- absorbing and were indistinguishable in morphology and size (Fig. 2A–C,F). Fig. 3 shows the absorbance data collected in this study. Fig. 3A–D shows the mean relative absorbance and Fig. 3E–H examples of unbleached (red line) and bleached (blue line) absorbance spectra for each class of cone (single cone measurements). The ultraviolet-sensitive cone absorbance spectra are shown in Fig. 3A,E. The mean λ_{max} for the α-band absorption was 371±9.2 nm (*N*=11) (see Table 1 for further spectral data on the ultraviolet-sensitive cones). The second class of single cones was the blue-sensitive cone shown in Fig. 2A-C,F. The mean λ_{max} for the α-band absorption band was 432±10.4 nm (*N*=29) (see Table 1 for spectral data and Fig. 3B,F for the absorbance curves of the blue-sensitive cones).

Double cones

All double cones recorded in this study were non-identical pairs having dissimilar spectral absorption properties: one red-sensitive and the other green-sensitive (see Fig. 2F). The mean λ_{max} for the α-band of the green-sensitive outer segments was 519±8.5 nm (*N*=25) (see Table 1 for spectral data and Fig. 3C,G for absorbance spectra of the green-sensitive cone outer segment of the double cones). The mean λ_{max} of the α-band of the red-sensitive outer segments differed for the sample of 14 double cones examined: 574±13.9 nm (*N*=6) and 623±17.9 nm (*N*=8) (See Table 1 for spectral data and Fig. 3D,H for the absorbance spectra of the red-sensitive outer segments of the double cones). Consistent with earlier observations (Hawryshyn and Hárosi, 1994), we found the double cones to be the most fragile photoreceptors encountered in our preparations, and they clearly exhibited signs of degeneration and decrease in visual pigment density well before the single cones and rods.

Rods

We measured 23 rod photoreceptors, and in this sample we were able to differentiate rhodopsin, porphyropsin and mixed A_1 and A_2 visual pigment spectra. In Fig. 4A–C we show the absorbance spectra for three classes of rod photoreceptors (see

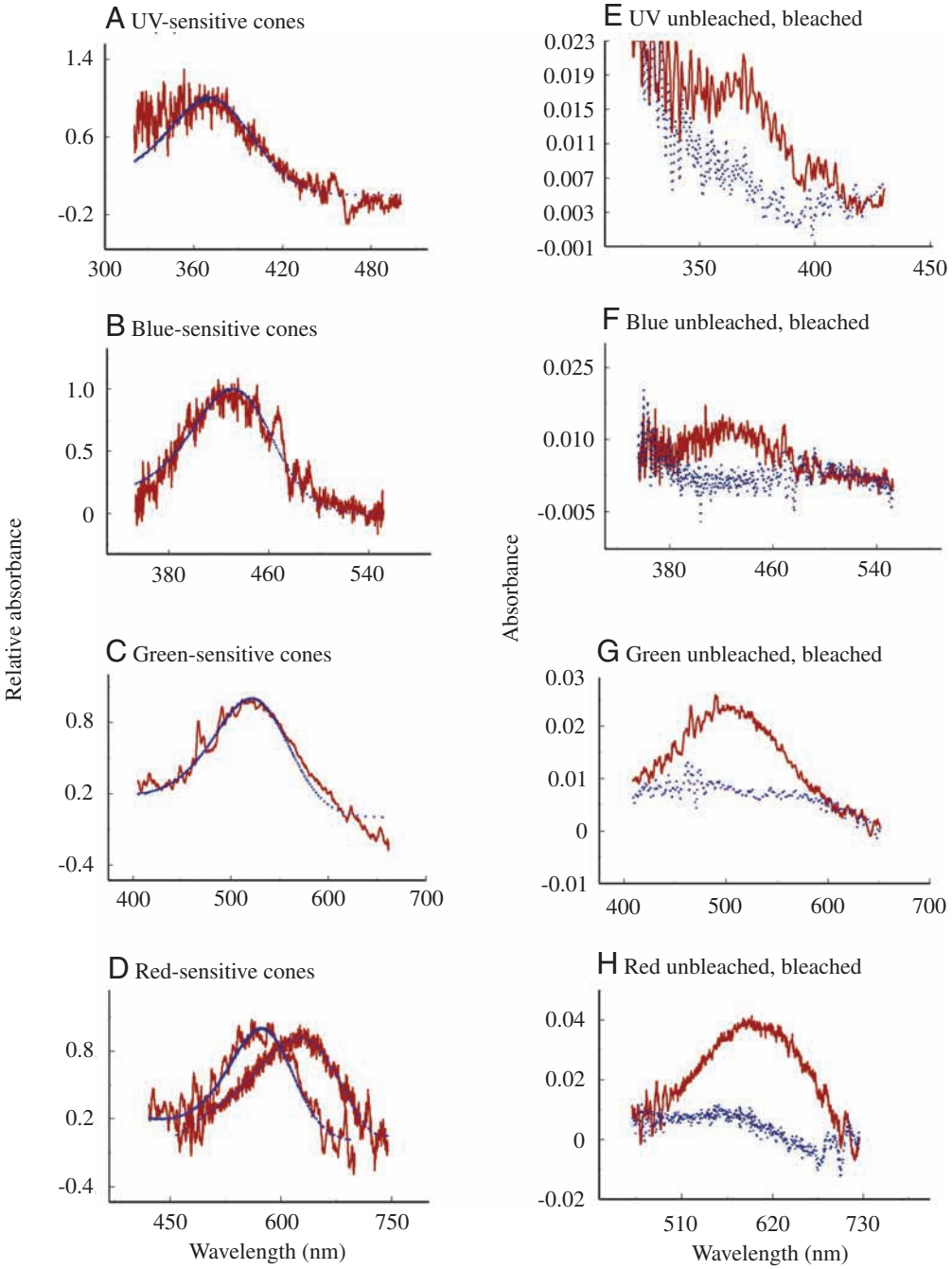

Fig. 3. Representative absorbance spectra of rainbow trout cone photoreceptors. (A–D) Mean relative absorbance for the ultraviolet- (A), blue- (B), green- (C) and red-sensitive cones (D, two spectra represent curves dominated by the A_1 and A_2 visual pigments). The red line shows the mean absorbance spectrum and the blue line shows the eighth-order polynomial template. Note that the two spectra (red lines) in D represent the A_1-based visual pigment red-sensitive cones (curve peaking at 574 nm) fitted by an eighth-order template and the A_2-based visual pigment red-sensitive cones (curve peaking at 623 nm) fitted by a Fourier transform function. (E–H) The unbleached (red line) and bleached (blue line) absorbance of a single cone recording for the ultraviolet- (E), blue- (F), green- (G) and red-sensitive (H) cones. See Table 1 for additional spectral data of cones.

Table 1 for spectral data). Table 1 shows three mean λ_{max} values of the α-band of rods: 504±2.1 nm (N=10, rhodopsin-dominated rods), 522±8.2 nm (N=5, porphyropsin-dominated rods) and 510±2.1 nm (N=8, rhodopsin porphyropsin mixed rods). Table 1 also shows that the half-maximum bandwidth (HBW, cm^{-1}) of the three absorbance spectra vary in a predictable manner, with the porphyropsin absorbance curve being wider than the rhodopsin absorbance spectrum and the mixed chromophore rods having the broadest absorbance spectrum. All spectra were fitted with long-wavelength limb templates derived from Munz and Beatty (Munz and Beatty; 1965) (100 % A_1, Fig. 4A; 50 % A_1: 50 % A_2, Fig. 4B and 100 % A_2 Fig. 4C) and the HBWs were determined using eighth-order polynomial templates (rhodopsin) and Fourier transform (porphyropsin and A_1/A_2 mixture absorbance curves). The absorbance spectra for the rods are slightly elevated in the short-wavelength portion of the spectrum due to photoproducts resulting from red light contamination within the dark room. This source of contamination has been identified and eliminated.

Discussion

In the present study, CCD-based MSP was used to measure the absorbance spectra of rainbow trout photoreceptors. Our primary goal was to evaluate the performance of our newly

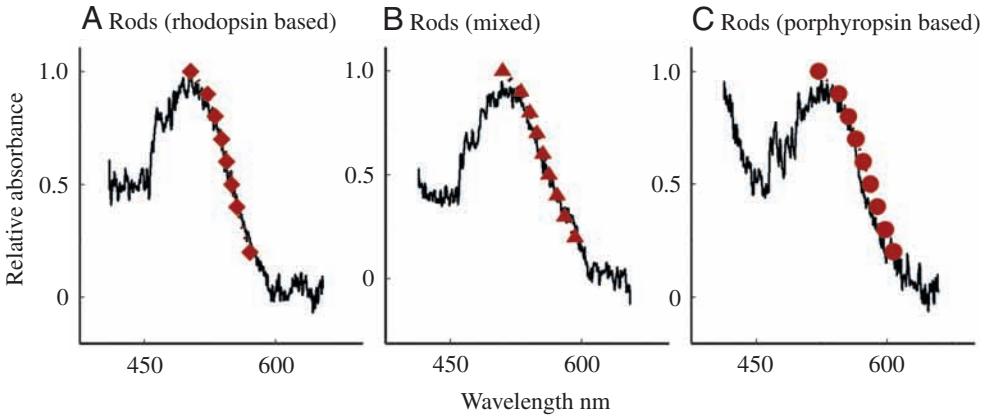

Fig. 4. Representative absorbance spectra of rainbow trout rod photoreceptors. (A) Mean absorbance spectrum of rhodopsin-based rods (black line). This spectrum (red diamonds) and those in B (red triangles) and C (red circles) are fitted with long-wavelength limb templates taken from Munz and Beatty (Munz and Beatty, 1965). (B) Mean absorbance spectrum for mixed rhodopsin porphyropsin rods. (C) Mean absorbance spectrum for porphyropsin-based rods.

designed CCD-based MSP by comparing our results with those of a previous study, which examined rainbow trout absorbance spectra using wavelength-scanning MSP (Hawryshyn and Hárosi, 1994). Data derived from the two different techniques compare favourably in λ_{max}, A_{max} and HBW. We believe that A_{max} was lower for the rods and longer-wavelength cones, compared to the earlier study (Hawryshyn and Hárosi, 1994) because of suspected red light contamination within the dark room. Some of the differences evident in the data are probably a reflection of the variable A_1/A_2 visual pigment ratios of the fish used in both studies. This was especially true for the ultraviolet-, blue- and green-sensitive cones. As Hárosi (Hárosi, 1994) points out, the relationship between λ_{max}, HBW of the α-absorption band and the A_1/A_2 ratio is not well understood for paired-pigment fishes (Hawryshyn and Hárosi, 1994). We were successful in resolving A_1 and A_2 visual pigment spectra for the rods and the red-sensitive cones but not for the ultraviolet-, blue- and green-sensitive cones. Clearly, further work is required to extend our analysis to the ultraviolet-, blue- and green-sensitive cones of salmonids (see Whitmore and Bowmaker, 1989). Govardovskii et al. (Govardovskii et al., 2000) has recently established universal templates for A_1- and A_2-based visual pigments; however, other works (most notably by Hárosi, 1994; MacNichol, 1986) have shown that universal templates do not necessarily account for all absorbance curves with λ_{max} values throughout the spectrum. One of our future objectives is to model the relationship between λ_{max} and HBW of the α-absorption band as a function of varying A_1/A_2 ratio for all photoreceptor classes, specifically in Pacific salmonid fishes, and test this model against empirical data collected from a broad range of salmonid species and life history stages. In the present study, we deliberately selected a wide size range of rainbow trout in an attempt to generate spectra that reflected A_1 and A_2 visual pigment differences. While our measurements on red-sensitive cones and rods provided data appropriate for this analysis, we did not see clear A_1 and A_2 visual pigment differences in the ultraviolet-, blue- and green-sensitive cones. We did see a slightly elevated variance in our estimates of λ_{max} and HBW in comparison with those of Hawryshyn and Hárosi (Hawryshyn and Hárosi, 1994), and this was to be expected since the rainbow trout used in the earlier study (Hawryshyn and Hárosi, 1994) were thought to have primarily A_1-based visual pigments. The absorbance spectra for the red-sensitive cones yielded two different mean λ_{max} values, indicative of A_1- (λ_{max} 574 nm) and A_2-based (λ_{max} 623 nm) visual pigments. Similarly, the rod absorbance spectra could be resolved into those conforming to A_1, A_2 and mixed A_1/A_2 visual pigment spectral properties (Fig. 4A–C). Using long-wavelength limb template-fitting, we have been able to determine the A_1/A_2 ratio of rods from a wide size range of rainbow trout to within 10 % of the A_1/A_2 ratio (not illustrated here). Further refinement of this technique of accurately estimating the A_1/A_2 ratio of rods will assist in determining the smoltification status of Pacific salmonid fishes (see Alexander et al., 1994; Alexander et al., 1998).

Prior to a seaward migration, anadromous salmonids (migrating from fresh water to sea water) change their visual pigment composition from a porphyropsin (freshwater visual pigment) to rhodopsin (marine visual pigment). Measurements of changing visual pigment composition of rods over time, together with changes in other physiological characteristics (silvering, modification of gill epithelia for purposes of osmoregulatory competence), are now being examined as tools for assessing the smoltification status of anadromous salmonid fishes. One aspect of our future research is to use visual pigment composition as an index of smoltification in an application that may have important implications for Salmonid Enhancement Programs (hatchery stocking) and the aquaculture industry.

While we are satisfied with the performance of the CCD-base MSP instrument described here, its development was challenging in a number of respects. The initial phase of development utilized an InstaSpec IV CCD system (Oriel), which lacked the sensitivity required to measure the low absorbance typical of vertebrate photoreceptors. We subsequently retrofitted a photointensifier (Generation II, Science Tech, London, Ontario); however, at low photon flux, we discovered that the multichannel plate intensifier introduced problematic levels of noise into the signal (Shot Noise). The back-illuminated CCD system (Roper Scientific) that we ultimately chose has very high sensitivity over the

range of 300–800 nm and chip-cooling maintains the noise at a low level. Such CCD systems now used in spectroscopy are more expensive than photomultipliers used in wavelength-scanning systems but, as with most electro-optical technology, we expect that CCD spectroscopy systems will be more cost-effective in the near future. The development of CCD-based MSP technology has been limited, to some extent, by developments in the electro-optical industry, but we are now satisfied with the performance of the system described here. Rapid data acquisition offers the advantages of less variance due to movement of target photoreceptors during measurement, reduced spectral distortion due to photoproduct interference and an ability to measure fast, transient changes in absorbance as bleaching proceeds. These factors contribute to low signal variance and offer CCD-based MSP as an attractive alternative to wavelength-scanning MSP.

Patrick Kerfoot and Gordon Davies provided excellent technical assistance. We would like to thank Ted Allison and Steve Dann for reading the manuscript and two anonymous referees for their insightful comments. Dr Cornelia Bohne kindly provided transmission spectra for neutral density filters used in the calibration of the apparatus. This research was funded by equipment and operating grants from the Natural Sciences and Engineering Research Council of Canada to C.W.H. and a Postdoctoral Fellowship from the Medical Research Council of Canada to M.E.D.

References

Alexander, G., Sweeting, R., McKeown, B. (1994). The shift in visual pigment dominance in the retinae of juvenile Coho Salmon (*Oncorhynchus kisutch*): an indicator of smolt status. *J. Exp. Biol*. **195**, 185–197.

Alexander, G., Sweeting, R., McKeown, B. (1998). The effect of thyroid hormone and thyroid hormone blocker on visual pigment shifting in juvenile salmon (*Oncorhynchus kisutch*). *Aquaculture* **168**, 157–168.

Avery, J. A., Bowmaker, J. K., Dzamgoz, M. B. A. and Downing, J. E. (1983). Ultraviolet sensitive receptors in a freshwater fish. *J. Physiol. Lond.* **334**, 23P.

Bernard, G. D. (1987). Spectral characterization of butterfly L-receptors using extended Dartnall/MacNichol. *J. Opt. Soc. Am. A* **4**, 123.

Bowmaker, J. M. (1984). Microspectrophotometry of vertebrate photoreceptors. *Vision Res*. **24**, 1641–1650.

Bowmaker, J. M. (1990). Visual pigments of fish. In *The Visual System of Fish* (ed. R. H. Douglas and M. B. A. Djamgoz), pp. 81–107. London: Chapman and Hall.

Bowmaker, J. M. (1995). The visual pigments in fish. In *Progress in Retinal and Eye Research,* vol. 15 (ed. N. N. Osborne and G. J. Chader), pp. 1–31. Oxford: Pergamon.

Bowmaker, J. M. and Kunz, Y. W. (1987). Ultraviolet receptors, tetrachromatic colour vision and retinal mosaics in the brown trout (*Salmo trutta*): age-dependent changes. *Vision Res*. **27**, 2102–2108.

Govardovskii, V. I., Fyhrquist, N., Reuter, T., Kuzmin, D. G. and Donner, K. (2000). In search of a visual pigment template. *Vis. Neurosci*. **17**, 509–528

Hárosi, F. I. (1987). Cynomolgus and rhesus monkey visual pigments: Application of Fourier Transform smoothing and statistical techniques to the determination of spectral parameters. *J. Gen. Physiol*. **89**, 717–743.

Hárosi, F. I. (1994). An analysis of two spectral properties of vertebrate visual pigments. *Vision Res*. **11**, 1359–1367.

Hárosi, F. I. and Hashimoto, Y. (1983). Ultraviolet visual pigment in a vertebrate: tetrachromatic cone system in the Dace. *Science* **222**, 1021–1023.

Hart, N. S., Partridge, J. C. and Cuthill, I. C. (1998). Visual pigments, oil droplets and cone photoreceptor distribution in the European starling (*Sturnus vulgaris*). *J. Exp. Biol*. **201**, 1433–1446.

Hawryshyn, C. W. and Hárosi, F. I. (1991). Ultraviolet photoreception in carp: Microspectrophotometry and behaviorally determined action spectra. *Vision Res*. **31**, 567–576.

Hawryshyn, C. W. and Hárosi, F. I. (1994). Spectral characteristics of visual pigments in rainbow trout (*Oncorhynchus mykiss*). *Vision Res*. **34**, 1385–1392.

Hiller-Adams, P., Widder, E. A. and Case, J. F. (1988). The visual pigments of four deep sea Crustacean species. *J. Comp. Physiol. A* **163**, 63–72.

Levine, J. S. and MacNichol, E. F., Jr (1985). Microspectrophotometry of primate photoreceptors: Art, artifact and analysis. In *The Visual System*, (ed. A. Fein and J. S. Levine), pp. 73–88. New York: Liss.

Liebman, P. A. (1972). Microspectrophotometry of photoreceptors. In *Handbook of Sensory Physiology*, vol. Vii/1 (ed. H. J. A. Dartnall), pp. 481–528. Berlin: Springer.

Liebman, P. A. and Entine, G. (1968). Visual pigments of frog and tadpole (*Rana pipiens*). *Vision Res*. **8**, 761–775.

Loew, E. R. (1995). Determinants of visual pigment spectral location and photoreceptor cell spectral sensitivity. In *Neurobiology and Clinical Aspects of the Outer Retina* (ed. M. B. A. Djamgoz, S. N. Archer and S. Vallerga), pp. 57–78. London: Chapman & Hall.

Loew, E. R. and Dartnall, H. J. A. (1976). Vitamin A_1/A_2-based visual pigment mixtures in cones of the rudd. *Vision Res*. **16**, 891–896.

Maier, E. J. and Bowmaker, J. K. (1993). Colour vision in the passiform bird *Leothrix lutea*: Correlation of visual pigment absorbance and oil droplet transmission with spectral sensitivity. *J. Comp. Physiol.* A, **172**, 295–301.

Maseide, K. and Rofstad, E. K. (1997). CCD imaging in cryospectrophotometric determination of microvascular oxyhemoglobin saturations. *Am. J. Physiol*. **273**, H2910–H2918.

Marks, W. B. (1965). Visual pigments in single goldfish cones. *J. Physiol. Lond*. **178**, 14–32.

Marks, W. B. and MacNichol, E. F., Jr (1962). Bleaching spectra of single goldfish cones. *Fed. Proc.* **519**, Abstract 2143.

MacNichol, E. F., Jr (1986). A unifying presentation of photopigment spectra. *Vision Res*. **26**, 1543–1556.

McFarland, W. N. and Loew, E. R. (1994). Ultraviolet visual pigments in marine fishes of the family pomacentridae. *Vision Res*. **34**, 1393–1396.

Munz, F. W. and Beatty, D. D. (1965). A critical analysis of the visual pigments of salmon and trout. *Vision Res*. **5**, 1–17.

Partridge, J. C. (1989). The visual ecology of avian oil droplets. *J. Comp. Physiol.* A **165**, 415–426.

Schweitzer, D., Hammer, M. and Scibor, M. (1996). Imaging spectrometry in ophthalmology – principle and applications in microcirculation and in investigation of pigments. *Ophthal. Res*. **28** (Suppl. 2), 37–44.

Sillman, A. J., Govardovskii, V.I., Röhlich, P., Southard, J. A. and Loew, E. R. (1997). The photoreceptors and visual pigments of the garter snake (*Thamnophis sirtalis*): a microspectrophotometric, scanning electron microscope and immunocytochemical study. *J. Comp. Physiol.* A **181**, 89–101.

Tang, Z., Ho, R., Xu, Z., Shao, Z. and Somlyo, A. P. (1994). A high-sensitivity CCD system for parallel electron energy-loss spectroscopy (CCD for EELS). *J. Microsc*. **175**, 100–107.

Tsujita, K., Shiraishi, T. and Kakinuma, K. (1997). Microspectrophotometry of nitric oxide-dependent changes in hemoglobin in single red blood cells incubated with stimulated macrophages. *J. Biochem*. **122**, 264–270.

Whitmore, A. V. and Bowmaker, J. K. (1989). Seasonal variation in cone sensitivity and short-wave absorbing visual pigments in rudd *Scardinius erythrophthalmus. J. Comp. Physiol.* A **166**, 103–115.

Widder, E. A., Hiller-Adams, P. and Case, J. F. (1987). A multichannel microspectrophotometer for visual pigment investigations. *Vision Res.* **27**, 1047–1055.